Oxidation of Metals, Vol. 14, No. 4, 1980

The Role of Thermal Shock in Cyclic Oxidation

Carl E. Lowell* and Daniel L. Deadmore*

Received March 22, 1979

The effect of thermal shock on the spalling of oxides from the surfaces of several commercial alloys was determined. The average cooling rate was varied from approximately 240°C/sec to less than 1.0°C/sec during cyclic oxidation tests in air. The tests consisted of 100 cycles of 1 hr at the maximimum temperature (1100 or 1200°C). The alloys were HOS-875, TD-Ni, TD-NiCrAl, In-601, In-702, and B-1900 plus Hf. All of these alloys exhibited partial spalling within the oxide rather than total oxide loss down to bare metal. Thermal shock resulted in deformation of the metal, which in turn resulted, in most cases, in change of the oxide failure mode from compressive to tensile. Tensile failures were characterized by cracking of the oxide and little loss, while compressive failures were characterized by explosive loss of platelets of oxide. This behavior was confirmed by examination of mechanically stressed oxide scales. The thermally shocked oxides spalled less than the slow-cooled samples with the exception of TD-NiCrAl. This material failed in a brittle manner rather than by plastic deformation. The HOS-875 and the TD-Ni did not spall during either type of cooling. Thus, the effect of thermal shock on spalling is determined, in large part, by the mechanical properties of the metal.

KEY WORDS: oxidation; cyclic; spalling; stress.

INTRODUCTION

When metals are cyclically oxidized, three phenomena control the rate of degradation of the material: (1) oxide growth; (2) oxide vaporization; and (3) oxide spalling. Oxide growth has been extensively investigated for a wide range of materials and this work has often been summarized, e.g., Kofstad[1]

*National Aeronautics and Space Administration, Lewis Research Center, Cleveland, Ohio.

0030-770X/80/0800-0325$03.00/0

and Hauffe.[2] However, most current high-temperature materials have relatively moderate rates of oxide formation[3] and the major modes of failure under normal use conditions are oxide vaporization and/or oxide spallation.[3,4] Oxide vaporization is a major problem only for those materials whose protective scales contain a substantial fraction of chromia (Cr_2O_3) and which are exposed to high-velocity gases. However, almost all materials systems suffer from oxide spalling regardless of gas velocity.

Oxide spalling has been the object of an increasing number of investigations in recent years and several comprehensive survey papers have been produced, e.g., Hancock and Hurst[5] and Douglass.[6] These surveys pointed out that far more work has been devoted to oxide growth stresses than to cyclically induced stresses. The latter have been given little attention even though they are generally assumed to be the cause of oxide spalling. These cyclic stresses are generally assumed to arise from coefficient of thermal expansion (CTE) mismatch between oxide and metal. The effects of cooling rate, cycle frequency, and other cyclic variables have been largely ignored.

Instead, much spalling work has focused on the oxide–metal interface and the effect of additions such as La, Y, etc., on the oxide–metal bond.[7–9] This work has shown that when high-purity NiAl, NiCrAl, and FeCrAl alloys are oxidized, voids form at the oxide–metal interface, which can lead to extensive spalling to bare metal. The addition of Y or other reactive metals at small concentrations can effectively prevent the void formation and hence spalling to bare metal. While these additions greatly reduce oxide spalling, they do not completely eliminate it. Spalling within the oxide still occurs and, while the rate of loss is diminished, it still can be a significant effect. Further, recent work in the Ni–Cr–Al system[10] has shown that small amounts of Zr have the same effect as Y. Since zirconium or other tramp elements are present in most commercially produced alloys, one would expect that such alloys would not exhibit bare-metal spalling. Therefore, the importance of Y and similar additions is probably restricted to overlay coatings which tend to be of high purity by the nature of their deposition processes. Indeed, cyclic oxidation of a large number of alloys has tended to confirm this view (Ref. 3 and unpublished NASA data).

The work reported in this paper is a continuation of an effort to establish the relative importance of cyclic oxidation variables in the degradation rate of metals and alloys. Previous work[11] had established that CTE mismatch was a major influence on oxide spalling. The objective of the current investigation was to determine the effect of thermal shock on oxide spalling. Thermal shock is defined as a rapid temperature change. In these experiments rapid cooling was used. The effect of such rapid cooling in oxides is to set up thermal gradients which can lead to strains as the cooler outer layers try to contract and are restrained by the hotter interior of the

materials. If the strains are large enough, failure will occur. To test for the effects of thermal shock, metal coupons were cyclically oxidized in two sets of tests with the tests differing in cooling rate by about three orders of magnitude. The rapid cooling rate was faster than would be anticipated in any application and the slow cooling rate was the slowest practical. Differences in the results of the two types of test were judged by weight change as a function of cycles. The materials examined were commercially produced and known not to spall to bare metal during cyclic oxidation.

MATERIALS

The compositions of the alloys used in these tests are shown in Table I. All but TD-Ni were used in the CTE mismatch work of Ref. 11. Both TD-NiCrAl and HOS-875 are alumina formers, while TD-Ni forms NiO. IN-702 and IN-601 are nickel-base wrought alloys; the former relies on alumina-aluminate and the latter on chromia for oxidation protection. Finally, B-1900 + Hf is a cast nickel-base alloy which forms a complex scale of Al_2O_3, spinels, HfO_2, and several other oxides during oxidation. The samples were machined to approximately $2.5 \times 1.3 \times 0.2$ cm. Before oxidation the samples were rinsed in ethyl alcohol, swabbed off, and air dried.

Cyclic oxidation was carried out in the apparatus shown in Fig. 1. The furnace can be raised or lowered by a variable speed motor between

Table I. Alloy Analysis, wt.%

Element	HOS 875[a]	TDNi[a]	TDNiCrAl[b]	IN-702[a]	IN-601[b]	B-1900[a] + Hf
Chromium	22.15	0.01	16.22	15.6	23.04	8.0
Aluminum	5.39	—	4.63	3.4	1.38	6.0
Iron	Bal.	<0.01	—	0.4	13.41	<0.35
Nickel	—	Bal.	Bal.	Bal.	Bal.	Bal.
Cobalt	—	<0.01	—	—	—	10.5
Molybdenum	—	—	—	—	—	6.0
Niobium	—	—	—	—	—	<0.10
Tantalum	—	—	—	—	—	4.25
Hafnium	—	—	—	—	—	1.60
Titanium	—	<0.001	—	0.7	—	1.0
Silicon	—	—	—	0.2	0.48	<0.25
Manganese	—	—	—	0.05	0.27	<0.2
Boron	—	—	—	—	—	0.015
Carbon	—	0.004	—	0.05	0.04	0.10
Thorium	—	2.0[c]	1.78[c]	—	—	—

[a]Typical analysis.
[b]Analysis for this heat.
[c]Present as ThO_2.

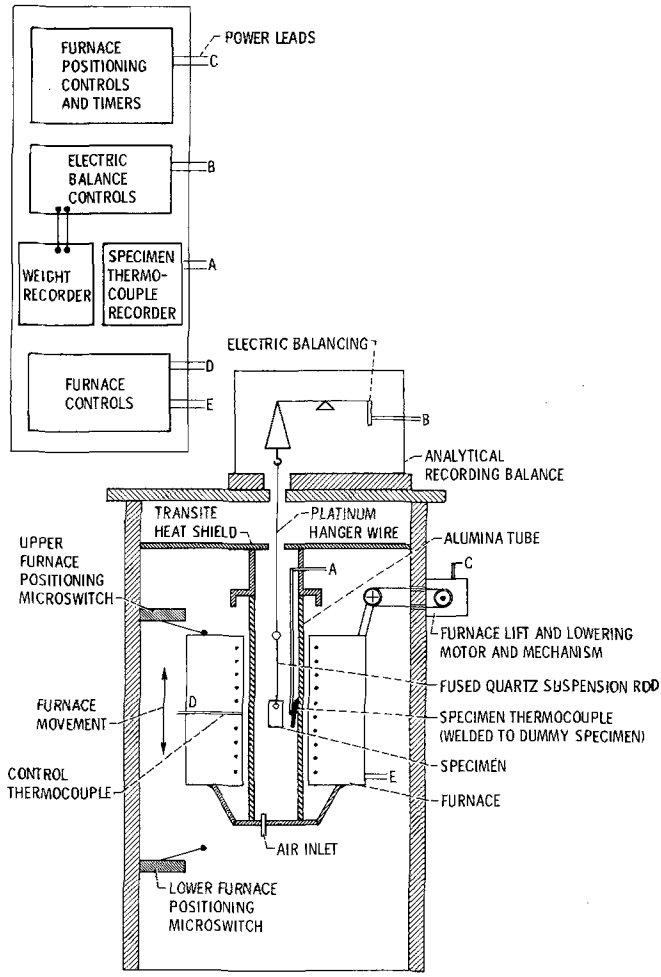

Fig. 1. Continuous weight change, cyclic oxidation apparatus for use at ambient pressure.

adjustable limit switches. At the start of the test, the furnace is lowered and the sample suspended from the balance. A dummy sample with a thermocouple is positioned next to, but not touching the sample. The furnace is heated to the oxidizing temperature and the test started by raising the furnace until the sample is in the center of the hot zone. The temperature is controlled to within $\pm 5°C$. At the end of the cycle, the furnace was lowered very slowly in one set of tests. For rapid cooling, the sample was taken from the furnace and plunged into water; oil and liquid nitrogen were also tried

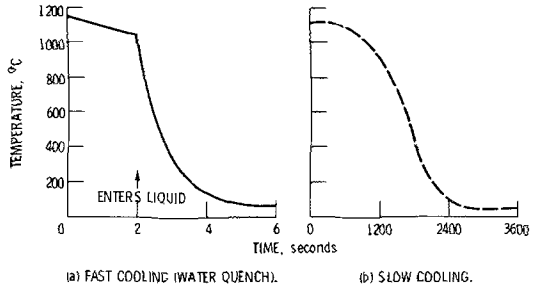

Fig. 2. Typical cooling curves.

but found to result in slower cooling rates. These cycles were then repeated until the completion of the runs. The slow-cooled samples were weighed continuously but the fast-cooled samples were removed from the water, rinsed in ethyl alcohol, and then weighed.

The cooling cycles for the two tests are shown in Fig. 2. The fast-cooling curve starts to cool relatively slowly as the sample is removed from the furnace, but the rate is dramatically accelerated when the sample enters the water. Total time to reach ambient temperature is about 5 sec. In contrast, the slow cooling cycle takes about 3000 sec to reach ambient temperature.

At the conclusion of each test, the samples were photographed and the retained oxide phases were determined by X-ray diffraction. Scanning electron microscopy was used to observe the surface morphology of the oxides and the samples were then sectioned and examined metallographically.

RESULTS

Specific Weight Change

Neither HOS-875 nor TD-Ni showed any significant effect of cooling rate on weight change during cyclic oxidation. The data for these materials are presented graphically in Fig. 3. In both cases, the weight-change curves are approximately the same as one would expect from an isothermal test, indicating that little if any spalling occurred at either cooling rate. B-1900, IN-601, and IN-702 all had smaller weight loss when rapidly cooled than when slowly cooled. This would imply that the thermal shock effect was not detrimental, i.e., did not increase spalling. In fact, the thermal shock seemed in some way beneficial. The only alloy whose weight-change data showed a large thermal shock contribution to spalling was TD-NiCrAl. This alloy showed a significant increase in cyclic weight loss when rapidly cooled as compared to the slow-cooling tests. This alloy had the least ductility of any tested. The significance of this fact will be discussed further below.

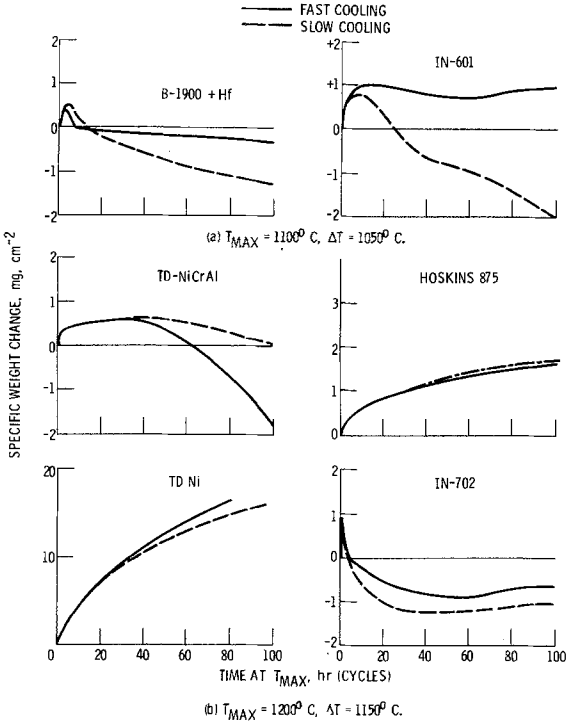

Fig. 3. The effect of cooling rate on the cyclic oxidation of some high-temperature alloys, 1 hr at T_{MAX} and $\frac{1}{2}$ hr at T_{MIN} per cycle.

Metal Distortion

One thing that was apparent in the fast-cooling tests was that the alloy coupons became more and more distorted as the tests progressed. Examples of such distortion are shown in Fig. 4. The wrought alloys HOS-875, TD-Ni, IN-702, and IN-601 all plastically deformed extensively, while cast B-1900 + Hf had considerably less, but measurable plastic deformation. These alloys all tended to elongate and assume a dogbone shape, although the HOS-875, the weakest alloy, also curled (Fig. 4b). In contrast, the alloy with very limited ductility (TD-NiCrAl) had little plastic deformation, and cracked extensively (Fig. 4a).

It was assumed that the cause of the deformation was the rapid cooling and not oxidation. To test this assumption a coupon of IN-601 was put into an 1100°C furnace just long enough to reach temperatures (~1 min), removed, and plunged into water. After a few such thermal cycles, thermal growth was noted. By the end of 40 cycles the change was quite obvious, as can be seen in Fig. 5.

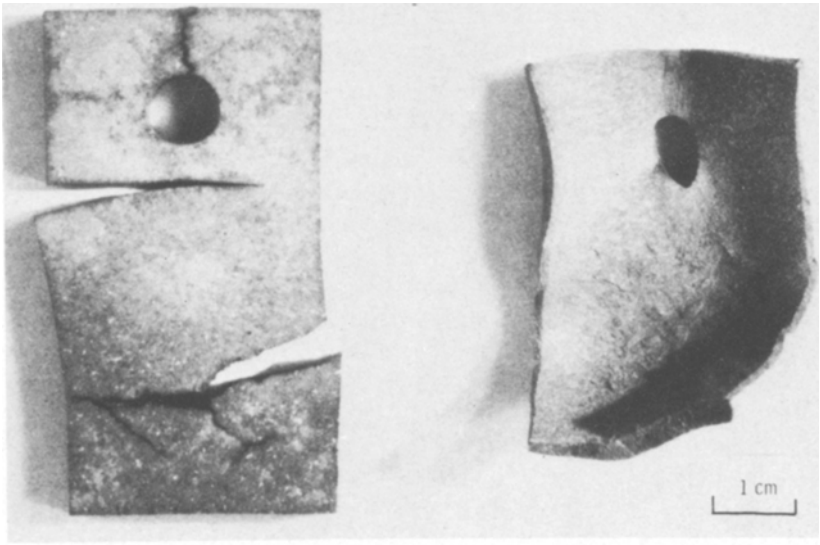

Fig. 4. Deformation modes of thermal shock after 80 1-hr cycles.

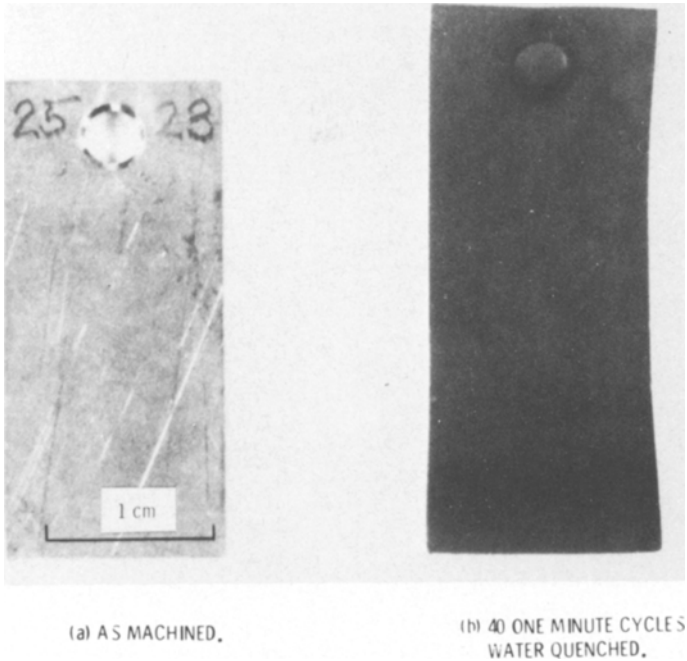

Fig. 5. Metal flow from thermal shock—IN-601.

SURFACE MORPHOLOGY

A comparison of the slow-cooled oxide surface morphologies with those of rapidly cooled oxides was made using scanning electron microscopy. Of particular interest were the surfaces on IN-702, IN-601, and B-1900+Hf. Figure 6 shows the comparison for IN–702. The oxide morphology of the air-cooled sample is typical of the type of spalling which normally occurs on cooling. It results from CTE mismatch-induced compressive stresses in the oxide exceeding the strength of the oxide. When this happens, large flakes of oxide part from the scale, often explosively. In the case of the rapidly cooled sample the oxide appears to have failed by cracking, but there is no evidence of the loss of large oxide flakes of oxides. Furthermore, the crack pattern is nearly a regular array much as one might expect from a biaxial tensile failure.

In an attempt to reproduce these surface oxide morphologies under more controlled stress conditions, a coupon of TD Ni (Approximately $4 \times 1.6 \times 0.3$ cm) was oxidized at 1200°C for 100 hr and slowly cooled. As there is virtually no CTE mismatch between Ni and NiO, cooling the sample resulted in an almost stress-free, unspalled oxide layer. The sample was then bent along the 4 cm length to a 2.5 cm radius. This resulted in a compressive stress in the NiO on the concave face and a tensile stress in the NiO on the convex face. The sample surfaces were evaluated in the scanning electron microscope and then sectioned and examined metallographically. The results are seen in Fig. 7. On the compression face, large oxide flakes have spalled much the same as the oxide on IN-702 after slow cooling (Fig. 6a). The failures occur along planes approximately parallel to the oxide–metal

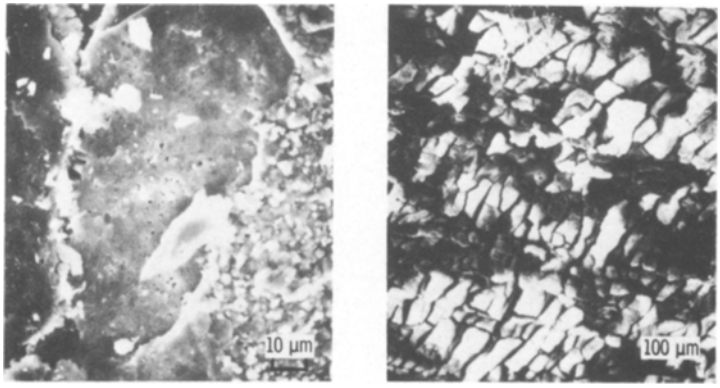

(a) IN-702 AIR COOLED. (b) IN-702 WATER QUENCHED.

Fig. 6. Effect of cooling rate on oxide surface structure of a ductile alloy.

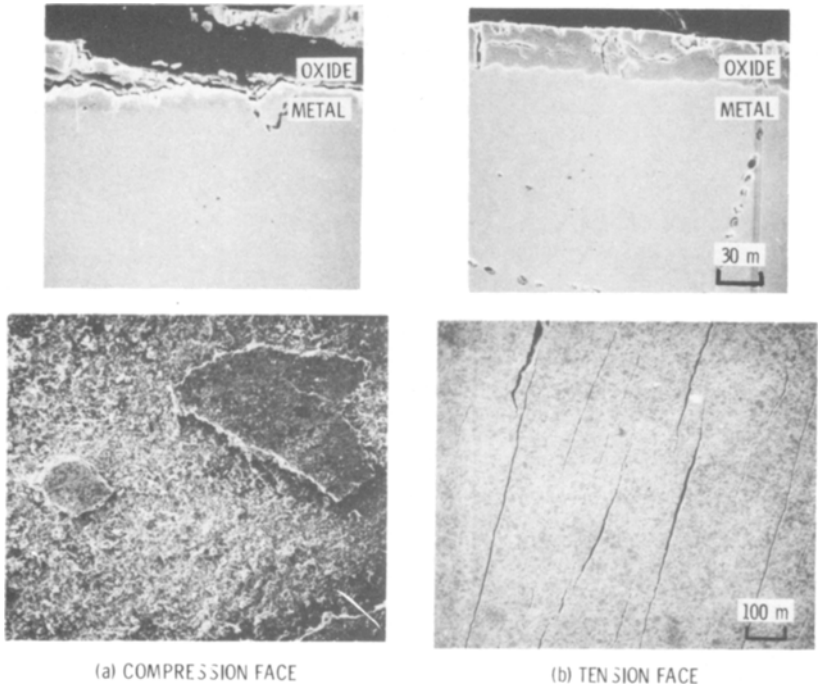

Fig. 7. NiO failure modes.

interface but are wholly within the oxide. On the tension face, the failure is primarily perpendicular to the oxide–metal interface, takes place largely as cracks normal to the tensile axis, and does not result in spalling. Comparison with the fast-cooled surface of IN-702 (Fig. 6b) again reveals a marked similarity except that the IN-702 tensile stress appears to be biaxial.

DISCUSSION

Metal Deformation

It is quite clear that, aside from the effects on spalling, thermal shock has a major effect on the metal itself: deformation. The source of this deformation can be seen schematically in Fig. 8. At temperature, the sample is a parallelepiped under no stress. As the sample is rapidly cooled, it cools from the surface inward and a temperature gradient is induced. The outer surface tries to contract but is constrained by the hotter interior; this sets up a tensile stress in the surface layers with a compressive stress inside. If the tensile stress is great enough, the surface will deform. With time, the thermal

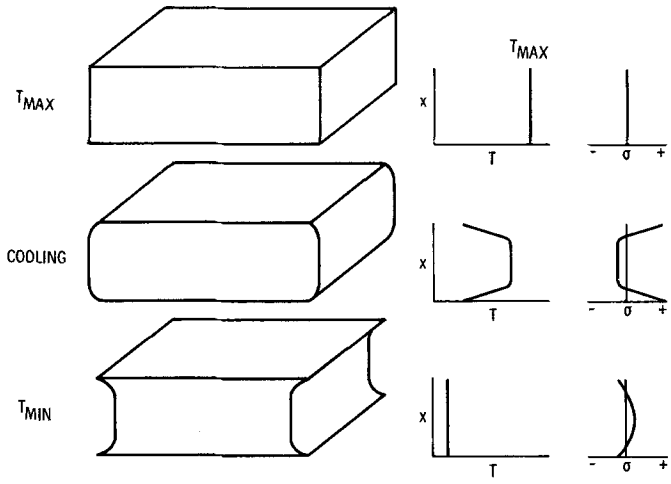

Fig. 8. Thermal shock in a ductile alloy—schematic.

gradient disappears as the entire sample reaches ambient temperature. Then with plastic flow, the stresses are reversed. Depending on the size of the stresses and the strength of the alloy, this can result in either the eared sample shape shown in Fig. 8 or a more uniform increase in length and width. In either case, this must obviously be accompanied by a reduction in thickness. The length change has the apparent effect of reducing the CTE of the sample. It should also be pointed out that this phenomenon, depending on its extent, may adversely affect attempts to use thickness change as a measure of the extent of oxidation. In some cases one might even measure thickness increases.

In the case of brittle samples, such as TD-NiCrAl, plastic deformation of the metal cannot occur and the sample simply breaks leaving the apparent CTE the same in the uncracked areas as without rapid cooling.

Tensile and Compressive Oxide Failure

With the metal deformation modes in hand, we are now ready to interpret the weight-change data observed as affected by cooling rate. We will use the schematic spalling diagram shown in Fig. 9. The sequence outlined on the left-hand side represents the usual spalling failure mechanism. At temperature, the oxide is under either no stress or slight growth stress. As the sample slowly cools, the oxide develops a compressive stress from CTE mismatch (the oxide contracts less than the metal) which increases with further cooling. As the stress exceeds the strength of the oxide, an explosive failure of the oxide takes place which results in a thinner

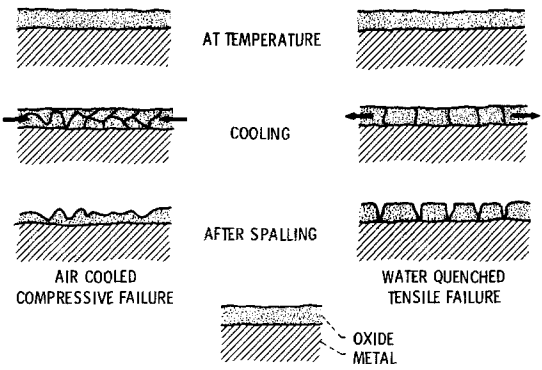

Fig. 9. Schematic representation of the effect of cooling rate on spalling.

protective oxide. On subsequent cycles, this scenario is repeated and leads ultimately to catastrophic metal loss.

If a ductile metal is rapidly cooled, the sequence on the right-hand side of Fig. 9 is followed. As before, zero or slight growth stresses are present in the oxide at temperature. If the metal is stressed sufficiently on rapid cooling (as is apparently the case for IN-702, IN-601, and B-1900 + Hf), the metal at the metal–oxide interface will plastically deform, greatly decreasing its apparent CTE to a value less than that of the oxide. This results in a tensile stress in the oxide. The stress is relieved by cracking the oxide but no loss of oxide is observed. This results in a much lower oxide formation rate during subsequent oxidation cycles and a smaller weight loss.

Of the two processes outlined above, the slow-cooling scenario is more prevalent in oxidation testing. Even in experiments or applications in which rapid cooling occurs, cooling rates seldom approach those achieved in these tests. Therefore, even when the effects of thermal shock are present, they are usually small compared to the usual error and are seldom apparent. Two exceptions might be burner rig testing where the samples are cooled with a high-velocity air jet and high frequency cyclic furnace testing. In the latter case, the thermal shock deformation in the metal, while small for each cycle, is cumulative and may eventually become significant. In any event, it is clear that CTE mismatch has far more influence on spalling than thermal shock.

CONCLUSIONS

By comparing the influence of rapid and slow cooling on cyclic oxidation of several commercial alloys, the following conclusions can be reached:

1. The way in which thermal shock affects spalling is by deformation of the metal at the oxide–metal interface.

2. Whether thermal shock increases or decreases spalling depends on the mechanical properties of the metal.

3. CTE mismatch is a more important influence on spalling than thermal shock.

4. Metal deformation resulting from thermal shock can severely limit the use of metal thickness-change data as a criterion for the extent of metal consumed during cyclic oxidation.

REFERENCES

1. P. Kofstad, *High-Temperature Oxidation of Metals* (Wiley, New York, 1966).
2. K. Hauffe, *Oxidation of Metals* (Plenum, New York, 1965).
3. C. A. Barrett and C. E. Lowell, *Oxid. Met.* **9**, 307 (1975).
4. C. E. Lowell and W. A. Sanders, *Oxid. Met.* **5**, 221 (1972).
5. P. Hancock and R. C. Hurst, in *Advances in Corrosion Science and Technology*, Vol. 4, R. W. Staehle and M. G. Fontana, eds. (Plenum, New York, 1974).
6. D. L. Douglass, *Oxidation of Metals and Alloys* (American Society for Metals, Metals Park, Ohio, 1971), p. 137.
7. J. L. Smialek, "Oxide Morphology and Spalling Model for NiAl," *Metall. Trans. A*, **9A**, 309 (1978).
8. C. S. Giggins and F. S. Pettit, "Oxide Scale Adherence Mechanism," ARL TR 75-0234 (June 1975).
9. F. A. Golightly, F. H. Stott, and G. C. Wood, *Oxid. Met.* **10**, 163 (1976).
10. C. A. Barrett and C. E. Lowell, *Oxid. Met.* **11**, 199 (1977).
11. D. L. Deadmore and C. E. Lowell, *Oxid. Met.* **11**, 91 (1977).